

A Low-Complexity Design for IRS-Assisted Secure Dual-Function Radar-Communication System

Yi-Kai Li, *Member, IEEE* and Athina Petropulu, *Fellow, IEEE*

Abstract—In dual-function radar-communication (DFRC) systems the probing signal contains information intended for the communication users, which makes that information vulnerable to eavesdropping by the targets. We study the security of a DFRC system aided by an intelligent reflecting surface (IRS) from the physical layer security (PLS) perspective. The IRS helps overcome path loss or blockage and introduces more degrees of freedom for system design, however, it also makes the design problem more challenging. In the system considered, the radar embeds artificial noise (AN) in the probing waveform, and the radar waveform, the AN noise and the IRS parameters are designed to optimize the communication secrecy rate while meeting radar signal-to-noise ratio (SNR) constraints. The contribution of the paper is a novel, low complexity approach to solve the underlying optimization problem and obtain the design parameters. In particular, we consider an alternating optimization approach, where in each iteration, the problem is decomposed into two sub-problems, namely, one that designs the IRS parameters, and another that jointly designs the radar waveform and the AN. The challenges in those sub-problems are the fractional objective, the SNR being a quartic function of the IRS parameters, and the unit-modulus constraint on the IRS parameters. A fractional programming technique is used to transform the fractional form objective into a more tractable non-fractional polynomial form. A closed-form based approach is proposed for the IRS design problem, which results in low complexity IRS design. Numerical results are provided to demonstrate the convergence properties of the proposed system design method, the secrecy rate and beamforming performance of the designed system.

Index Terms—DFRC, physical layer security, IRS, low-complexity design

I. INTRODUCTION

Integrated sensing and communication (ISAC) systems aim to perform both sensing and communication functions from a common platform [2]–[5]. An ISAC system can sense the physical environment and also transmit communication signals, which greatly benefits unmanned aerial vehicles (UAV) networks [6], extended reality (XR) applications [7], ultra-reliable and low-latency communications (URLLC) [8], and autonomous vehicles [9]. A subclass of ISAC systems is the Dual-Function Radar-Communication (DFRC) systems, which, in addition to providing a common platform for both

communication and sensing, utilize a shared waveform [10]–[12]. In DFRC systems, user information is embedded in the probing waveform, resulting in higher spectral efficiency as compared to general ISAC systems. However, this also raises security concerns as the embedded communication information can be intercepted by a target which is also an eavesdropper (ED). This paper studies the security of DFRC systems from a physical layer security (PLS) perspective.

In wireless communications, the PLS design aims to leverage the physical characteristics of the wireless channel to degrade the quality of the signal received by the ED [13]–[20]. One approach to ensure PLS is cooperative jamming, where trusted relays act as helpers and beamform artificial noise (AN), aiming to degrade the ED’s channel [14]–[18]. Another approach is to embed AN in the signal intended for the users, in a way that it does not create interference to the users [19], [20]. PLS design for DFRC systems has been considered in [21], [22], where the DFRC system embeds AN in the transmit waveform, and a radar beamformer and the AN are jointly designed to minimize the ED signal-to-noise-ratio (SNR) [21], or maximize the weighted normalized Fisher information matrix determinant and normalized secrecy rate [22].

A DFRC system can be enhanced via the use of intelligent reflecting surfaces (IRS). The IRS is a planar array of passive elements, each of which can alter the phase of the incoming electromagnetic wave in a computer-controlled manner. These elements can cooperatively perform beamforming to increase the power that is radiated towards intended directions, or decrease it towards unintended directions. The IRS can assist the DFRC system in overcoming performance limitations caused by path loss or blockage, which are likely to arise in the next-generation wireless systems due to the use of high frequencies. The IRS can also create additional links between the radar and the users, or between the radar and the targets, thus introducing more degrees of freedom (DoFs) for system design [23]–[27]. When there is no line-of-sight (LoS) between the radar and the target, which is also the case considered in this paper, the IRS can provide alternative paths for the radar signal to reach the target [23], [25].

In this paper, we investigate the design for an IRS-aided secure DFRC system from the PLS perspective. The radar transmits a precoded waveform along with additive precoded AN. The radar waveform, the AN noise and the IRS parameters are designed to optimize the communication secrecy rate while meeting radar SNR constraints. The IRS parameter is a diagonal matrix containing the responses of the IRS elements. We consider passive IRS elements, i.e., elements that only change the phase of the impinging signal. Therefore, each non-zero element of the IRS parameter matrix is subject to unit

This work was presented in part in 2023 IEEE Asilomar Conference on Signals, Systems, and Computers [1]. This work is supported by ARO grant W911NF2320103 and NSF grant ECCS-2320568.

Athina Petropulu is with the Electrical and Computer Engineering Department, Rutgers, the State University of New Jersey, NJ, USA 08854 (e-mail: athinap@rutgers.edu).

Yi-Kai Li is with the Department of Electrical and Computer Engineering and Technology, Minnesota State University Mankato, MN, USA 56001 (e-mail: yikai.li@mnsu.edu).

modulus constraint (UMC). Here, we consider the scenario where there is no LoS between the radar and the target. The signal transmitted by the radar reaches the target after reflection upon the IRS, and subsequently returns to the radar after reflection upon the IRS [28]. Thereby, the radar SNR is a non-convex fourth order function of the IRS parameter. Since the design variables are highly coupled with each other, we solve the optimization problem via an iterative optimization framework where, in each iteration, we first solve for the waveform and the AN by taking the IRS parameters as fixed (first sub-problem), and then find the IRS parameters with the previously computed values for the waveform and the AN (second sub-problem). The first sub-problem can be easily formulated as a quadratic programming problem. On the other hand, the second sub-problem is more challenging due to the non-convex fractional form of the secrecy rate objective, the non-convex high-order radar SNR, and the UMC on the IRS parameter.

In our preliminary work [1], we address the aforementioned second sub-problem via a classical semidefinite relaxation (SDR) method. We express the non-convex high-order radar SNR term as a quadratic function of an auxiliary variable, which is quadratic in the IRS parameter. Subsequently, via the minorization maximization (MM) technique [29], we replace the SNR with a lower bound that is linear in the auxiliary variable. To address the non-convex fractional objective of secrecy rate and achieve a tractable design problem we invoke a fractional programming technique [30]. Subsequently, all functions in the objective and constraints are non-fractional quadratic functions of the IRS parameter, and the transformed problem is solved via an SDR method. The quadratic functions of the IRS parameter are transformed into functions of the Gram of the IRS parameter, and the Gram matrix is obtained via the interior point method (IPM). However, in [1] the UMC on the IRS parameter is relaxed during the optimization process, and the obtained solution is retracted to the unit complex circle to ensure feasibility. The retracted solution does not necessarily satisfy the radar SNR constraint, and at the same time leads to approximation loss. Thus, multiple solutions need to be generated to obtain a satisfactory one. The complexity of the approach of [1] is $\mathcal{O}(N^{4.5})$. When large size IRS is desired to reap high array gain [31], such complexity becomes prohibitive.

To circumvent the IPM, we propose a novel closed-form expression-based IRS update method. Firstly, the high order and fractional functions of the IRS parameter in the problem are transformed into linear functions. Specifically, the radar SNR, is converted into a linear function of the IRS parameter by applying the MM [29] twice [32]. The secrecy rate objective is first transformed into a quadratic non-fractional function via the quadratic transform [30], and then it is converted into a linear function via the MM method [29]. As such, the IRS parameter design problem becomes a linear programming (LP) problem subject to UMC. This problem can be solved by solving the corresponding Lagrangian dual problem, which has a closed-form solution in each iteration [33]. The Lagrangian multiplier in the dual problem can be found by a bi-section search. [33] introduced a method for

non-fractional quadratic constrained quadratic programming (QCQP) under UMC, without incorporating high-order or fractional functions. [33] also provided a case study on hybrid beamforming design utilizing their proposed solution. As compared to [33] we propose a novel closed form expression by leveraging a solution that accommodates UMC in a different context. Unlike [1], in the proposed approach, the UMC is always satisfied during the optimization process.

Relation to the literature The literature on striking a balance between PLS and sensing performance for IRS-aided DFRC systems is in its early stages. In [34]–[41], the waveform design problems are formulated as quadratic programming problems. In [34], the waveform is designed by applying Courant’s penalty method, and the IRS is optimized by utilizing distance-majorization. In [35], a penalty-based algorithm is used in the waveform design problem, where auxiliary variables are defined, and the violation of the defined linear relationship between the original and auxiliary variables becomes a penalization term incorporated to the objective. The IRS design in [35] is accomplished via MM. In [36], the design of the waveform and IRS parameter is done via SDR and MM, respectively. In [37], a penalization term is integrated to the objective to penalize the violation of the rank-one constraints of the Gram matrices of the design variables. In [38], the design of IRS-aided secure DFRC system is completed by the MATLAB build-in *fmincon* function. In [39], the Dinkelbach’s transform [42] is used to transform the waveform and IRS design problems to solvable non-fractional quadratic semi-definite programming (SDP) problems. In [40], the waveform design problem is convexified by a fractional programming technique, and the IRS parameter is obtained by applying the MM. In [41], the waveform design is convexified by a first-order Taylor series approximation, and the IRS is designed by a numerical simultaneous perturbation stochastic approximation method.

However, as in [1], the IRS design in most of the aforementioned methods [36]–[41] are based on IPM or numerical methods, which are computationally intensive when the IRS size is large. Our paper proposes a closed-form expression based method to enable a scalable IRS design algorithm. For those that also have a closed-form expression solution [34], [35] for the IRS design, [34] studies a different scenario, i.e., symbol-level precoding for secure IRS DFRC system. The metrics involved in the design problem are non-fractional quadratic functions. Our proposed method addresses optimization problem containing high order and fractional functions of the IRS parameters. In [35], the authors focus on the problem of maximizing the beampattern gain towards the target subject to minimum SINR at the user and maximum allowed information leakage to the target/ED, which is a different problem as compared to our paper. Moreover, [35] concentrates on the metric of beampattern gain towards the target without addressing secrecy rate, while our paper involves the secrecy rate at the user, the SNR at radar receiver, and the obtained beampatterns under different system configurations. In addition to the aforementioned methods, deep reinforcement learning (DRL) [43] have been used to optimize the secrecy rate of IRS-aided DFRC system [44]. However, the dimension-

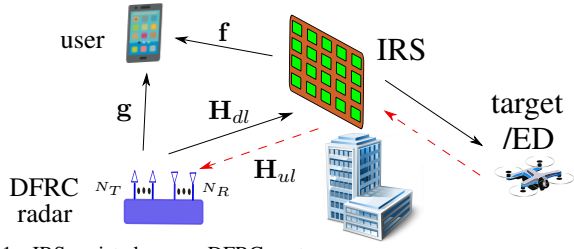


Fig. 1. IRS-assisted secure DFRC system.

ality of the agent's search space, specifically the configured phases of the IRS elements, expands exponentially as the size of the IRS increases. Consequently, DRL algorithms might exhibit a slower rate of convergence in scenarios where the IRS is large.

II. SYSTEM MODEL

We consider an IRS-aided DFRC system, as show in Fig. 1, where the DFRC is communicating with a user while simultaneously tracking a non-line-of-sight (NLoS) target. We consider such NLoS case as that case necessitates the use of an IRS for target sensing. The target is not authorized to access the communication information, so it will be treated as ED. The DFRC transmitter is an N_T -antenna uniform linear array (ULA), and the DFRC receiver is a collocated N_R -antenna ULA array. The inter-antenna distance in both arrays is denoted by d . Both the user and the ED are equipped with a single antenna. An N -element IRS is deployed to aid both the sensing and communication functionalities. The channels are assumed flat fading and the channel coefficients are assumed to be available. In DFRC systems, the channels can be estimated by leveraging the sensing function [45], [46]. Here we assume perfect channel knowledge, however, in simulations we demonstrate the effects of channel errors on the system performance.

The signal transmitted by the DFRC radar is the sum of the precoded signal intended for the communication user, s , and the precoded AN, \mathbf{n} , i.e.,

$$\mathbf{x} = \mathbf{w}s + \mathbf{W}_n\mathbf{n}, \quad (1)$$

where $\mathbf{w} \in \mathbb{C}^{N_T \times 1}$ denotes the precoder for s and $\mathbf{W}_n \in \mathbb{C}^{N_T \times N_T}$ the precoder for \mathbf{n} . Here, s is assumed to be zero-mean white, with unit variance; $\mathbf{n} \sim \mathcal{CN}(\mathbf{0}_{N_T \times 1}, \sigma^2 \mathbf{I}_{N_T})$. The AN is used for jamming but also helps in the detection of the target/ED.

Since there is no LoS between the radar and the target, the transmitted waveform arrives at the target via the DFRC-IRS-target path, and the target echo reaches the radar receiver via the target-IRS-DFRC path. The signal at the radar receiver is

$$\begin{aligned} y_R &= \alpha_T \beta \mathbf{H}_{ul} \Phi \mathbf{a}_I(\psi_a, \psi_e) \mathbf{a}_I^T(\psi_a, \psi_e) \Phi \mathbf{H}_{dl} (\mathbf{w}s + \mathbf{W}_n\mathbf{n}) + \mathbf{n}_R \\ &= \mathbf{C}_T (\mathbf{w}s + \mathbf{W}_n\mathbf{n}) + \mathbf{n}_R, \end{aligned} \quad (2)$$

where α_T represents the radar target reflection coefficient; β is the combined effect of the attenuation of DFRC-IRS-target-IRS-DFRC path, the antenna gain, and any additional losses or gains; \mathbf{H}_{ul} and \mathbf{H}_{dl} are the normalized IRS-DFRC and DFRC-IRS channels, respectively; $\Phi = \text{diag}([e^{j\phi_1}, e^{j\phi_2}, \dots, e^{j\phi_N}])$ represents the IRS parameter matrix, with $\phi_n \in [0, 2\pi)$

denoting the phase shift of the n -th IRS element; $\mathbf{a}_I(\psi_a, \psi_e)$ is the steering vector of the IRS, with ψ_a and ψ_e denoting the azimuth and elevation angles of the target relative to the IRS, respectively; $\mathbf{n}_R \sim \mathcal{CN}(\mathbf{0}_{N_R \times 1}, \sigma_R^2 \mathbf{I}_{N_R})$ represents additive white Gaussian noise (AWGN) at the DFRC receiving array.

The SNR at the radar receiver for detecting the target is

$$\gamma_R = \text{tr}[\mathbf{C}_T [\mathbf{w}\mathbf{w}^H + \mathbf{W}_n\mathbf{W}_n^H] \mathbf{C}_T^H] / \sigma_R^2. \quad (3)$$

The received signal at the communication user is

$$\begin{aligned} y_u &= (\mathbf{g}^T + \beta_H^{\frac{1}{2}} \mathbf{f}^T \Phi \mathbf{H}_{dl}) (\mathbf{w}s + \mathbf{W}_n\mathbf{n}) + n_u \\ &= \mathbf{c}_u^T (\mathbf{w}s + \mathbf{W}_n\mathbf{n}) + n_u, \end{aligned} \quad (4)$$

where $\mathbf{g} \in \mathbb{C}^{N_T \times 1}$ is the channel between the user and DFRC transmitter; β_H is the path-loss of the DFRC-IRS channel; $\mathbf{f} \in \mathbb{C}^{N \times 1}$ denotes the user-IRS channel; $n_u \sim \mathcal{CN}(0, \sigma_u^2)$ is AWGN at the user.

The received signal at the target/ED is

$$\begin{aligned} y_{te} &= (\beta^{\frac{1}{2}} \mathbf{a}_I^T(\psi_a, \psi_e) \Phi \mathbf{H}_{dl}) (\mathbf{w}s + \mathbf{W}_n\mathbf{n}) + n_{te} \\ &= \mathbf{c}_{te}^T (\mathbf{w}s + \mathbf{W}_n\mathbf{n}) + n_{te}, \end{aligned} \quad (5)$$

where $n_{te} \sim \mathcal{CN}(0, \sigma_{te}^2)$ is AWGN at the target/ED.

The achievable rates at the user and target/ED are respectively

$$R_u = \log(1 + \text{SINR}_u) = \log\left(1 + \frac{|\mathbf{c}_u^T \mathbf{w}|^2}{\|\mathbf{c}_u^T \mathbf{W}_n\|^2 + \sigma_u^2}\right), \quad (6)$$

$$R_{te} = \log(1 + \text{SINR}_{te}) = \log\left(1 + \frac{|\mathbf{c}_{te}^T \mathbf{w}|^2}{\|\mathbf{c}_{te}^T \mathbf{W}_n\|^2 + \sigma_{te}^2}\right). \quad (7)$$

III. SYSTEM DESIGN

We consider the design of the radar information precoder, \mathbf{w} , the artificial noise precoder, \mathbf{W}_n , and the IRS parameter matrix, Φ , as that of maximizing the secrecy rate, defined as $(R_u - R_{te})$, while satisfying certain constraints, i.e.,

$$(\mathbb{P}) \quad \max_{\mathbf{w}, \mathbf{W}_n, \Phi} \quad R_u - R_{te} \quad (8a)$$

$$\text{s.t.} \quad \text{tr}[\mathbf{w}\mathbf{w}^H + \mathbf{W}_n\mathbf{W}_n^H] \leq P_R \quad (8b)$$

$$|\Phi_{n,n}| = 1, \quad \forall n = 1, \dots, N \quad (8c)$$

$$\gamma_R \geq \gamma_{R,th} \quad (8d)$$

where (8b) enforces that the total power of the transmitted signal stays below P_R ; (8c) enforces unit modules elements in Φ . This is because the IRS is composed of passive elements, which can only change the phase of the impinging signal; (8d) ensures that the radar SNR is above threshold $\gamma_{R,th}$.

Remark In the following we will assume that the target/ED angle is known. However, it does not need to be known exactly, and only an initial estimate would suffice. As long as the target will fall within the beam that will be formulated by the proposed system, it will be detected and its angle will be fine-tuned. The new angle will be used in the subsequent communication/sensing phase. In this way, the proposed DFRC will be able to track moving targets.

The problem (\mathbb{P}) in (8) is challenging for the following reasons: (i) The design variables, \mathbf{w} , \mathbf{W}_n , Φ , are mutually coupled. (ii) The objective is the difference between two non-convex functions (R_u and R_{te}), and is non-convex. (iii) The

radar SNR in (8d), γ_R , is quartic in Φ . Since γ_R is quadratic in \mathbf{C}_T (see (3)), and \mathbf{C}_T is second order in Φ (see (2)). (iv) Φ is subject to highly non-convex UMC.

To decouple the design variables, we divide the problem (8) into two sub-problems. The first one is optimization with respect to \mathbf{w} and \mathbf{W}_n for fixed Φ , and the second one is optimization with respect to Φ for fixed \mathbf{w} and \mathbf{W}_n . These two sub-problems are solved in an alternating way until a convergence condition is met [47].

A. First sub-problem: Solve for \mathbf{w} and \mathbf{W}_n for fixed Φ

The first sub-problem is formulated as follows:

$$(\mathbb{P}_1) \quad \max_{\mathbf{w}, \mathbf{W}_n} \quad R_u - R_{te} \quad (9a)$$

$$\text{s.t.} \quad \text{tr}[\mathbf{w}\mathbf{w}^H + \mathbf{W}_n \mathbf{W}_n^H] \leq P_R \quad (9b)$$

$$\gamma_R \geq \gamma_{R,th} \quad (9c)$$

Note that R_u , R_{te} are both fractional forms of the design variables. Here, we invoke the quadratic transform technique [30] to recast R_u and R_{te} into non-fractional functions of \mathbf{w} and \mathbf{W}_n . Thereby, the problem (\mathbb{P}_1) becomes a non-fractional quadratic programming problem. The Lagrangian dual expressions of R_u and R_{te} in (6) and (7) are

$$\begin{aligned} R_u &= (1 + \gamma_u) |\mathbf{c}_u^T \mathbf{w}|^2 / (|\mathbf{c}_u^T \mathbf{w}|^2 + \|\mathbf{c}_u^T \mathbf{W}_n\|^2 + \sigma_u^2) - \gamma_u \\ &+ \log(1 + \gamma_u) = -\alpha_u^2 (|\mathbf{c}_u^T \mathbf{w}|^2 + \|\mathbf{c}_u^T \mathbf{W}_n\|^2 + \sigma_u^2) \\ &+ 2\alpha_u \sqrt{1 + \gamma_u} |\mathbf{c}_u^T \mathbf{w}| + \log(1 + \gamma_u) - \gamma_u, \end{aligned} \quad (10)$$

$$\begin{aligned} R_{te} &= (1 + \gamma_{te}) |\mathbf{c}_{te}^T \mathbf{w}|^2 / (|\mathbf{c}_{te}^T \mathbf{w}|^2 + \|\mathbf{c}_{te}^T \mathbf{W}_n\|^2 + \sigma_{te}^2) - \gamma_{te} \\ &+ \log(1 + \gamma_{te}) = -\alpha_{te}^2 (|\mathbf{c}_{te}^T \mathbf{w}|^2 + \|\mathbf{c}_{te}^T \mathbf{W}_n\|^2 + \sigma_{te}^2) \\ &+ 2\alpha_{te} \sqrt{1 + \gamma_{te}} |\mathbf{c}_{te}^T \mathbf{w}| + \log(1 + \gamma_{te}) - \gamma_{te}, \end{aligned} \quad (11)$$

where γ_u , α_u , γ_{te} , and α_{te} are auxiliary variables, whose values are updated in each iteration. The derivation details of (10) and (11) are provided in Appendix (A). Then, the objective can be re-written as

$$R_u - R_{te} = c + \Re(\mathbf{v}^T \mathbf{w}) + \text{tr}[\mathbf{M}(\mathbf{W}_n \mathbf{W}_n^H + \mathbf{w}\mathbf{w}^H)], \quad (12)$$

where

$$c = \log(1 + \gamma_u) - \gamma_u - \log(1 + \gamma_{te}) + \gamma_{te} + \alpha_{te}^2 \sigma_{te}^2 - \alpha_u^2 \sigma_u^2, \quad (13)$$

$$\mathbf{v} = 2\alpha_u \sqrt{1 + \gamma_u} \mathbf{c}_u - 2\alpha_{te} \sqrt{1 + \gamma_{te}} \mathbf{c}_{te}, \quad (14)$$

$$\mathbf{M} = \alpha_{te}^2 \mathbf{c}_{te}^* \mathbf{c}_{te}^T - \alpha_u^2 \mathbf{c}_u^* \mathbf{c}_u^T. \quad (15)$$

The above is a quadratic programming problem with non-fractional objective and constraints and can be solved via SDR. By letting $\mathbf{R}_w = \mathbf{w}\mathbf{w}^H$ and $\mathbf{R}_{W_n} = \mathbf{W}_n \mathbf{W}_n^H$, the Problem (\mathbb{P}_1) in (9) becomes

$$(\overline{\mathbb{P}}_1) \quad \max_{\mathbf{w}, \mathbf{R}_w, \mathbf{R}_{W_n}} \quad \Re(\mathbf{v}^T \mathbf{w}) + \text{tr}[\mathbf{M}(\mathbf{R}_{W_n} + \mathbf{R}_w)] + c \quad (16a)$$

$$\text{s.t.} \quad \text{tr}[\mathbf{R}_w + \mathbf{R}_{W_n}] \leq P_R \quad (16b)$$

$$\text{tr}[\mathbf{C}_T^H \mathbf{C}_T (\mathbf{R}_w + \mathbf{R}_{W_n})] / \sigma_{R,th}^2 \geq \gamma_{R,th} \quad (16c)$$

$$\mathbf{R}_w \succcurlyeq \mathbf{w}\mathbf{w}^H \quad (16d)$$

where c is irrelevant to the design variables, and thus can be dropped, and \mathbf{R}_w and \mathbf{R}_{W_n} are positive semidefinite matrices.

¹This constraint can not be directly accepted in CVX toolbox [48] for $N > 1$, and is relaxed to an inequality as (16d).

The Problem ($\overline{\mathbb{P}}_1$) in (16) is an LP problem, whose optimal solution, say \mathbf{w}^* and $\mathbf{R}_{W_n}^*$, can be obtained by numerical solvers, for example by using the CVX toolbox [48]. The optimal solution for \mathbf{W}_n is obtained by calculating the square root matrix of $\mathbf{R}_{W_n}^*$.

B. Second sub-problem: Solve for Φ for fixed \mathbf{w} and \mathbf{W}_n

The design problem of IRS parameter, Φ , is as follows

$$(\mathbb{P}_2) \quad \max_{\Phi} \quad R_u - R_{te} \quad (17a)$$

$$\text{s.t.} \quad |\Phi_{n,n}| = 1, \quad \forall n = 1, \dots, N \quad (17b)$$

$$\gamma_R \geq \gamma_{R,th} \quad (17c)$$

Besides the fractional form objective, the problem (\mathbb{P}_2) in (17) is subject to the challenging non-convex UMC on Φ as shown in (17b). Moreover, the γ_R in (17c) is a non-convex fourth order function of Φ . This term needs to be convexified to make the problem solvable.

We rewrite the effective channel for the user as

$$\begin{aligned} \mathbf{c}_u^T &= \mathbf{g}^T + \beta_H^{\frac{1}{2}} \mathbf{f}^T \Phi \mathbf{H}_{dl} = \mathbf{g}^T + \phi^T \beta_H^{\frac{1}{2}} \text{diag}(\mathbf{f}) \mathbf{H}_{dl} \\ &= \mathbf{g}^T + \phi^T \mathbf{D}, \end{aligned} \quad (18)$$

where $\phi = \text{diag}(\Phi)$ is the column vector that contains all diagonal elements of Φ , and $\mathbf{D} = \beta_H^{\frac{1}{2}} \text{diag}(\mathbf{f}) \mathbf{H}_{dl}$. Similarly, the effective channel for the ED/target is re-written as

$$\begin{aligned} \mathbf{c}_{te}^T &= \beta_I^{\frac{1}{2}} \mathbf{a}_I^T(\psi_a, \psi_e) \Phi \mathbf{H}_{dl} = \phi^T \beta_I^{\frac{1}{2}} \text{diag}(\mathbf{a}_I(\psi_a, \psi_e)) \mathbf{H}_{dl} \\ &= \phi^T \mathbf{E}, \end{aligned} \quad (19)$$

where $\mathbf{E} = \beta_I^{\frac{1}{2}} \text{diag}(\mathbf{a}_I(\psi_a, \psi_e)) \mathbf{H}_{dl}$. By invoking (14), (18), and (19), the first term in the transformed non-fractional objective in (16), $\Re(\mathbf{v}^T \mathbf{w})$, can be re-written as

$$\Re(\mathbf{v}^T \mathbf{w}) = \Re(\phi^T \boldsymbol{\eta}) + c_1, \quad (20)$$

where

$$\boldsymbol{\eta} = 2(\alpha_u \sqrt{1 + \gamma_u} \mathbf{D} - \alpha_{te} \sqrt{1 + \gamma_{te}} \mathbf{E}) \mathbf{w}, \quad (21)$$

$$c_1 = 2\Re(\alpha_u \sqrt{1 + \gamma_u} \mathbf{g}^T \mathbf{w}). \quad (22)$$

Furthermore, c_1 is taken as a constant in the second sub-problem. Likewise, by referring to (15), (18), and (19), the second item of the converted objective in (16), $\text{tr}[\mathbf{M}\mathbf{R}_{W_n}]$, is re-expressed as

$$\begin{aligned} \text{tr}[\mathbf{M}\mathbf{R}_{W_n}] &= \alpha_{te}^2 \mathbf{c}_{te}^T \mathbf{W}_n \mathbf{W}_n^H \mathbf{c}_{te}^* - \alpha_u^2 \mathbf{c}_u^T \mathbf{W}_n \mathbf{W}_n^H \mathbf{c}_u^* \\ &= \phi^T \mathbf{L}_1 \phi^* - \Re(\phi^T \boldsymbol{\mu}) - c_2, \end{aligned} \quad (23)$$

where

$$\mathbf{L}_1 = \alpha_{te}^2 \mathbf{E} \mathbf{W}_n \mathbf{W}_n^H \mathbf{E}^H - \alpha_u^2 \mathbf{D} \mathbf{W}_n \mathbf{W}_n^H \mathbf{D}^H, \quad (24)$$

$$\boldsymbol{\mu} = 2\alpha_u^2 \mathbf{D} \mathbf{W}_n \mathbf{W}_n^H \mathbf{g}^*, \quad (25)$$

$$c_2 = \alpha_u^2 \mathbf{g}^T \mathbf{W}_n \mathbf{W}_n^H \mathbf{g}^*. \quad (26)$$

Likewise, c_2 is taken as a constant in the design of Φ or ϕ . Similarly, $\text{tr}[\mathbf{M}\mathbf{R}_w]$ can be re-written as

$$\text{tr}[\mathbf{M}\mathbf{R}_w] = \phi^T \overline{\mathbf{L}}_1 \phi^* - \Re(\phi^T \overline{\boldsymbol{\mu}}) - \overline{c}_2, \quad (27)$$

where

$$\bar{\mathbf{L}}_1 = \alpha_{t_e}^2 \mathbf{E} \mathbf{w} \mathbf{w}^H \mathbf{E}^H - \alpha_u^2 \mathbf{D} \mathbf{w} \mathbf{w}^H \mathbf{D}^H, \quad (28)$$

$$\bar{\boldsymbol{\mu}} = 2\alpha_u^2 \mathbf{D} \mathbf{w} \mathbf{w}^H \mathbf{g}^*, \quad (29)$$

$$\bar{c}_2 = \alpha_u^2 \mathbf{g}^T \mathbf{w} \mathbf{w}^H \mathbf{g}^*. \quad (30)$$

Thereby, the objective, $R_u - R_{te}$ can be re-written as

$$\begin{aligned} R_u - R_{te} &= \Re(\mathbf{v}^T \mathbf{w}) + \text{tr}[\mathbf{M}(\mathbf{R}_{W_n} + \mathbf{R}_w)] + c \\ &= \phi^T (\mathbf{L}_1 + \bar{\mathbf{L}}_1) \phi^* + \Re[\phi^T (\boldsymbol{\eta} - \boldsymbol{\mu} - \bar{\boldsymbol{\mu}})] + \text{const}, \end{aligned} \quad (31)$$

which is a quadratic function of ϕ .

Next, we need to transform the radar SNR, γ_R , in (17c) to make (\mathbb{P}_2) solvable. Recall that the radar channel is $\mathbf{C}_T = \beta \mathbf{H}_{ul} \Phi \mathbf{a}_I(\psi_a, \psi_e) \mathbf{a}_I^T(\psi_a, \psi_e) \Phi \mathbf{H}_{dl}$. By denoting $\mathbf{U} = \Phi \mathbf{a}_I(\psi_a, \psi_e) \mathbf{a}_I^T(\psi_a, \psi_e) \Phi$, γ_R can be re-arranged as

$$\begin{aligned} \gamma_R &= \text{tr}[\mathbf{C}_T^H \mathbf{C}_T [\mathbf{w} \mathbf{w}^H + \mathbf{W}_n \mathbf{W}_n^H]] / \sigma_R^2 \\ &= \beta^2 / \sigma_R^2 \text{tr}[\mathbf{U}^H \mathbf{H}_{ul}^H \mathbf{H}_{ul} \mathbf{U} \mathbf{H}_{dl} (\mathbf{w} \mathbf{w}^H + \mathbf{W}_n \mathbf{W}_n^H) \mathbf{H}_{dl}^H] \\ &\stackrel{(a)}{=} \beta^2 / \sigma_R^2 \mathbf{u}^H \mathbf{Z} \mathbf{u}, \end{aligned} \quad (32)$$

where in step (a), $\text{tr}[\mathbf{U}^H \mathbf{A} \mathbf{U} \mathbf{B} \mathbf{U}^T] = \mathbf{u}^H (\mathbf{B} \otimes \mathbf{A}) \mathbf{u}$ is referred to, $\mathbf{Z} = [\mathbf{H}_{dl} (\mathbf{w} \mathbf{w}^H + \mathbf{W}_n \mathbf{W}_n^H) \mathbf{H}_{dl}^H]^T \otimes (\mathbf{H}_{ul}^H \mathbf{H}_{ul})$, and $\mathbf{u} = \text{vec}(\mathbf{U})$. Note that both \mathbf{U} and \mathbf{u} are quadratic in Φ or ϕ . To create a lower bound for γ_R that is quadratic in ϕ , we need to have a bound which is linear in \mathbf{u} . For this we invoke MM [29] as

$$\begin{aligned} \gamma_R &= \beta^2 / \sigma_R^2 \mathbf{u}^H \mathbf{Z} \mathbf{u} \\ &\geq \tilde{\gamma}_R = \beta^2 / \sigma_R^2 (\mathbf{u}^H \mathbf{Z} \mathbf{u}_t + \mathbf{u}_t^H \mathbf{Z} \mathbf{u} - \mathbf{u}_t^H \mathbf{Z} \mathbf{u}_t), \end{aligned} \quad (33)$$

where $\mathbf{u}_t = \text{vec}[\Phi_t \mathbf{a}_I(\psi_a, \psi_e) \mathbf{a}_I^T(\psi_a, \psi_e) \Phi_t]$, where Φ_t is the solution of Φ in t -th/previous iteration, the current iteration index is $(t+1)$, and $\tilde{\gamma}_R$ is the surrogate function for γ_R . In addition, the first term of $\tilde{\gamma}_R$ is re-expressed as

$$\begin{aligned} \mathbf{u}^H \mathbf{Z} \mathbf{u}_t &\stackrel{(b)}{=} \text{vec}(\mathbf{U})^H \text{vec}(\mathbf{V}) = \text{tr}[\mathbf{U}^H \mathbf{V}] \\ &\stackrel{(c)}{=} \text{tr}[\Phi^H \mathbf{a}_I^*(\psi_a, \psi_e) \mathbf{a}_I^H(\psi_a, \psi_e) \Phi^H \mathbf{V}] \\ &= \phi^H \{[\mathbf{a}_I^*(\psi_a, \psi_e) \mathbf{a}_I^H(\psi_a, \psi_e)] \circ \mathbf{V}^T\} \phi^*, \end{aligned} \quad (34)$$

where $\mathbf{u} = \text{vec}(\mathbf{U})$; \mathbf{V} is set such that $\text{vec}(\mathbf{V}) = \mathbf{Z} \mathbf{u}_t$; $\mathbf{U} = \Phi \mathbf{a}_I(\psi_a, \psi_e) \mathbf{a}_I^T(\psi_a, \psi_e) \Phi$. Similarly, the second term in $\tilde{\gamma}_R$ can be re-written as

$$\mathbf{u}_t^H \mathbf{Z} \mathbf{u} = \phi^T \{[\mathbf{a}_I(\psi_a, \psi_e) \mathbf{a}_I^T(\psi_a, \psi_e)] \circ \mathbf{Y}^T\} \phi, \quad (35)$$

where the matrix \mathbf{Y} satisfies $\text{vec}(\mathbf{Y}) = \mathbf{Z}^T \mathbf{u}_t^*$. Thereby, $\tilde{\gamma}_R$ in (33) can be written as

$$\tilde{\gamma}_R = \phi^H \mathbf{L}_2 \phi^* + \phi^T \mathbf{L}_3 \phi - \beta^2 / \sigma_R^2 \mathbf{u}_t^H \mathbf{Z} \mathbf{u}_t, \quad (36)$$

where the third term is not relevant to the variable ϕ , and

$$\mathbf{L}_2 = \beta^2 / \sigma_R^2 \{[\mathbf{a}_I^*(\psi_a, \psi_e) \mathbf{a}_I^H(\psi_a, \psi_e)] \circ \mathbf{V}^T\}, \quad (37)$$

$$\mathbf{L}_3 = \beta^2 / \sigma_R^2 \{[\mathbf{a}_I(\psi_a, \psi_e) \mathbf{a}_I^T(\psi_a, \psi_e)] \circ \mathbf{Y}^T\}. \quad (38)$$

So far, the objective (17a) and constraint (17c) in (\mathbb{P}_2) are transformed into non-fractional quadratic form. By invoking (31) and (36), (\mathbb{P}_2) can be re-written as

$$(\bar{\mathbb{P}}_2) \quad \max_{\phi} \quad \phi^T (\mathbf{L}_1 + \bar{\mathbf{L}}_1) \phi^* + \Re[\phi^T (\boldsymbol{\eta} - \boldsymbol{\mu} - \bar{\boldsymbol{\mu}})] \quad (39a)$$

$$\text{s.t.} \quad |\phi_{n,1}| = 1, \quad \forall n = 1, \dots, N \quad (39b)$$

$$\phi^H \mathbf{L}_2 \phi^* + \phi^T \mathbf{L}_3 \phi \geq \gamma'_{R,th} \quad (39c)$$

where $\gamma'_{R,th} = \gamma_{R,th} + \beta^2 / \sigma_R^2 \mathbf{u}_t^H \mathbf{Z} \mathbf{u}_t$. Now, $(\bar{\mathbb{P}}_2)$ is a quadratic programming problem with UMC on the elements of the variable ϕ as (39b). $(\bar{\mathbb{P}}_2)$ can be solved via the SDR method by rewriting it as follows [1]:

$$(\bar{\bar{\mathbb{P}}}_2) \quad \max_{\mathbf{R}_1, \mathbf{R}_2, \phi} \quad \text{tr}[(\mathbf{L}_1 + \bar{\mathbf{L}}_1) \mathbf{R}_1^*] + \Re[\phi^T (\boldsymbol{\eta} - \boldsymbol{\mu} - \bar{\boldsymbol{\mu}})] \quad (40a)$$

$$\text{s.t.} \quad |[\mathbf{R}_1]_{n,n}| \leq 1, \quad \forall n = 1, \dots, N \quad (40b)$$

$$|[\mathbf{R}_2]_{n,n}| \leq 1, \quad \forall n = 1, \dots, N \quad (40c)$$

$$\text{tr}[\mathbf{L}_2 \mathbf{R}_2^*] + \text{tr}[\mathbf{L}_3 \mathbf{R}_2] \geq \gamma'_{R,th} \quad (40d)$$

$$\mathbf{R}_1 \succcurlyeq \phi \phi^H \quad (40e)$$

$$\mathbf{R}_2 \succcurlyeq \phi \phi^T \quad (40f)$$

where $\mathbf{R}_1 = \phi \phi^H$ and $\mathbf{R}_2 = \phi \phi^T$. The latter two assignments represent constraints on \mathbf{R}_1 and \mathbf{R}_2 which are not allowed in the CVX toolbox [48]. To make the problem (40) solvable in CVX, these two constraints are relaxed as matrix inequalities in (40e) and (40f). For example, (40e) means that $\mathbf{R}_1 - \phi \phi^H$ is a positive semidefinite matrix. To improve the performance, we can use Gaussian randomization to acquire the solution of ϕ . That is, we can generate multiple random vectors whose Gram is \mathbf{R}_1 then element-wise normalize them, and choose as the solution the vector that maximizes the objective (40a) while satisfying the constraint (40d). The obtained ϕ is substituted into sub-problem 1 of the next iteration. The overall optimization algorithm for jointly designing \mathbf{w} , \mathbf{W}_n and Φ , is summarized as Algorithm 1, where $\text{obj}^{(t+1)}$ is the objective, or secrecy rate ($R_u - R_{te}$), obtained in the $(t+1)$ -th iteration, and ε is the indicator of error tolerance. The quadratic transform [30] based IRS parameter update method presented in this section is referred to as "qtSDR" for short. In addition, to solve the design problem (8), we invoke qtSDR along with the waveform and AN design method proposed in Section III-A, as summarized in Algorithm 1.

IV. CLOSED-FORM EXPRESSION BASED LOW-COMPLEXITY IRS PARAMETER UPDATE SCHEME

The qtSDR approach, presented in the previous section relaxes the UMC constraint, which may lead to loss in the secrecy rate. Further, for solving $(\bar{\bar{\mathbb{P}}}_2)$ of (40) involves IPM for updating the IRS parameter ϕ . IPM has high complexity when the size of ϕ (N) is large, which hinders the scalability of qtSDR. To bypass the aforementioned drawbacks, in this section we propose a closed-form expression based method for updating ϕ in each iteration, that takes into account the UMC and has low-complexity.

Inside each iteration of the algorithm, at first we solve for the waveform and AN as the first sub-problem block of Algorithm 1 shows. Then in the second sub-problem block, we use a closed-form expression to update the values of the IRS parameters, and this expression will invoke the value of

Algorithm 1: Secrecy rate maximization via qtSDR.

Result: Return \mathbf{w} , \mathbf{W}_n and Φ .

Initialization: $\Phi = \Phi_0$, $\mathbf{w} = \mathbf{w}_0$, $\mathbf{W}_n = \mathbf{W}_{n,0}$,

 $\gamma_u = \gamma_{u,0}$, $\alpha_u = \alpha_{u,0}$, $\gamma_{te} = \gamma_{te,0}$, $\alpha_{te} = \alpha_{te,0}$,
 $t = 0$;

while (1) **do**
// Auxiliary variables update
 $\alpha_u = \sqrt{1 + \gamma_u} |\mathbf{c}_u^T \mathbf{w}| / (|\mathbf{c}_u^T \mathbf{w}|^2 + \|\mathbf{c}_u^T \mathbf{W}_n\|^2 + \sigma_u^2)$;

 $\gamma_u = |\mathbf{c}_u^T \mathbf{w}|^2 / (|\mathbf{c}_u^T \mathbf{W}_n\|^2 + \sigma_u^2)$;

 $\alpha_{te} = \sqrt{1 + \gamma_{te}} |\mathbf{c}_{te}^T \mathbf{w}| / (|\mathbf{c}_{te}^T \mathbf{w}|^2 + \|\mathbf{c}_{te}^T \mathbf{W}_n\|^2 + \sigma_{te}^2)$;

 $\gamma_{te} = |\mathbf{c}_{te}^T \mathbf{w}|^2 / (|\mathbf{c}_{te}^T \mathbf{W}_n\|^2 + \sigma_{te}^2)$;

// First sub-problem

Solve (\mathbb{P}_1) of (16) to obtain \mathbf{w} and \mathbf{R}_{W_n} ;

Obtain \mathbf{W}_n as the square root matrix of \mathbf{R}_{W_n} ;

// Second sub-problem via qtSDR

Substitute \mathbf{w} , \mathbf{W}_n , found in the first sub-problem
into the second sub-problem;

Obtain ϕ by solving $(\tilde{\mathbb{P}}_2)$ in (40);

 $\Phi = \text{diag}(\phi)$;

// Condition of termination
if $((t \geq t_{\max}) \parallel (|\text{obj}^{(t+1)} - \text{obj}^{(t)}| / \text{obj}^{(t)} \leq \varepsilon))$
then

| Break;

end
 $t = t + 1$;

end

the solved IRS parameters in previous outermost iteration. We denote the index of the outermost iteration as t .

MM methods enable new ways to convexify non-convex problems [29], [33], i.e. by creating tight convex lower/upper bounds of the original non-convex functions, and then iteratively maximizing/minimizing those bounds. In our problem, our aim is to maximize the secrecy rate (see (39a)), while keeping the SNR at the radar receiver above a threshold (see (39c)). Both (39a) and (39c) contain quadratic functions of ϕ . In addition, the UMC on the elements of IRS parameter in (39b) imposes more non-convexity to the problem of (39).

Firstly, by invoking MM [29], we create lower bounds for the quadratic functions in (39), which are linear in ϕ , i.e.,

$$\phi^T (\mathbf{L}_1 + \bar{\mathbf{L}}_1) \phi^* \geq \phi_t^T (\mathbf{L}_1 + \bar{\mathbf{L}}_1) \phi^* + \phi^T (\mathbf{L}_1 + \bar{\mathbf{L}}_1) \phi_t^* - \phi_t^T (\mathbf{L}_1 + \bar{\mathbf{L}}_1) \phi_t^*, \quad (41)$$

$$\phi^H \mathbf{L}_2 \phi^* \geq 2\phi_t^H \mathbf{L}_2 \phi^* - \phi_t^H \mathbf{L}_2 \phi_t^*, \quad (42)$$

$$\phi^T \mathbf{L}_3 \phi \geq 2\phi_t^T \mathbf{L}_3 \phi - \phi_t^T \mathbf{L}_3 \phi_t, \quad (43)$$

where the current iteration index is $t+1$, and ϕ_t is the obtained value for ϕ in the previous/ t -th outermost iteration.

Thereby, the problem $(\tilde{\mathbb{P}}_2)$ in (39) is re-reformulated as

$$(\tilde{\mathbb{P}}_2) \quad \max_{\phi} \quad \phi_t^T (\mathbf{L}_1 + \bar{\mathbf{L}}_1) \phi^* + \phi^T (\mathbf{L}_1 + \bar{\mathbf{L}}_1) \phi_t^* - \phi_t^T (\mathbf{L}_1 + \bar{\mathbf{L}}_1) \phi_t^* + \Re[\phi^T (\boldsymbol{\eta} - \boldsymbol{\mu} - \bar{\boldsymbol{\mu}})] \quad (44)$$

$$\text{s.t.} \quad |\phi_{n,1}| = 1, \quad \forall n = 1, \dots, N \quad (45)$$

$$2\phi_t^H \mathbf{L}_2 \phi^* - \phi_t^H \mathbf{L}_2 \phi_t^* + 2\phi_t^T \mathbf{L}_3 \phi - \phi_t^T \mathbf{L}_3 \phi_t \geq \gamma'_{R,th} \quad (46)$$

For notation simplicity, we denote the objective in (44) as $g_0(\phi)$, and

$$g_1(\phi) = 2\phi_t^H \mathbf{L}_2 \phi^* - \phi_t^H \mathbf{L}_2 \phi_t^* + 2\phi_t^T \mathbf{L}_3 \phi - \phi_t^T \mathbf{L}_3 \phi_t - \gamma'_{R,th}. \quad (47)$$

Thereby, the problem $(\tilde{\mathbb{P}}_2)$ can be re-written as

$$(\tilde{\mathbb{P}}_2) \quad \max_{\phi} \quad g_0(\phi) \quad (48a)$$

$$\text{s.t.} \quad |\phi_{n,1}| = 1, \quad \forall n = 1, \dots, N \quad (48b)$$

$$g_1(\phi) \geq 0 \quad (48c)$$

So far, we have obtained an LP problem subject to UMC similar to [33]. In [33], an objective minimization problem with upper bound constraints is studied, while in our paper an objective maximization problem with lower bound constraints is studied. Similar to [33], we formulate and solve the Lagrangian dual problem of the original LP problem with UMC as follows. The Lagrangian dual function of the problem in (48) can be written as

$$\mathcal{L}(\rho) = \max_{\phi \in \Omega} \Re[g_0(\phi) + \rho g_1(\phi)] \quad (49)$$

where $\Omega = \{\phi \in \mathbb{C}^N \mid |\phi_{n,1}| = 1, \forall n = 1, \dots, N\}$, ρ is the Lagrangian multiplier and non-negative. The Lagrangian dual problem of $(\tilde{\mathbb{P}}_2)$ is

$$L^* = \min_{\rho \geq 0} \mathcal{L}(\rho) \quad (50)$$

The Lagrangian $\mathcal{L}(\rho)$ in (49) is linear in ϕ noting that $g_0(\phi)$ and $g_1(\phi)$ are both linear functions of ϕ , therefore the optimal $\mathcal{L}(\rho)$ can be obtained by letting

$$\phi(\rho) = \exp[j \arg(\boldsymbol{\nu}(\rho) + \boldsymbol{\kappa}^*(\rho))], \quad (51)$$

where

$$\boldsymbol{\nu}(\rho) = \left(\phi_t^T (\mathbf{L}_1 + \bar{\mathbf{L}}_1) + 2\rho \phi_t^H \mathbf{L}_2 \right)^T, \quad (52)$$

$$\boldsymbol{\kappa}(\rho) = \left[\phi_t^H (\mathbf{L}_1 + \bar{\mathbf{L}}_1)^T + 2\rho \phi_t^T \mathbf{L}_3 + (\boldsymbol{\eta} - \boldsymbol{\mu} - \bar{\boldsymbol{\mu}})^T \right]^T. \quad (53)$$

The derivation of Eq. (51) can be found in Appendix (B). Notice that the IRS parameter vector ϕ is now a function of ρ . A properly chosen ρ can ensure that the objective $g_0(\phi(\rho))$ is maximized while the constraint $g_1(\phi(\rho)) \geq 0$ is satisfied.

The parameter ρ quantifies the importance of the radar SNR constraint. In each iteration, initially $\rho = 0$, indicating maximization of the objective $g_0(\phi(0))$ with respect to ϕ without considering the radar SNR constraint. If the obtained solution, say $\phi^*(0)$, satisfies $g_1(\phi^*(0)) \geq 0$, then ρ is set to 0 in the current iteration. In this case, the $\phi^*(0)$ is used as the solution of the IRS parameter in the current iteration. If $g_1(\phi^*(0)) < 0$, this means that the radar SNR constraint is not satisfied with the obtained solution and a positive ρ is necessary. If ρ is too large, the radar SNR constraint is given too much importance, which might consume too many DoFs of the system, thus making it impossible to meet the secrecy rate objective. In this case, we find an upper bound of ρ at first, say $\rho_{ub} = 2^x$, where x is the smallest integer that satisfies

$g_1(\phi(\rho_{ub})) = g_1(\phi(2^x)) \geq 0$. Then, a smallest ρ^* is found in the range of $(0, \rho_{ub})$ using the bisection method conditioned on $g_1(\phi(\rho^*)) \geq 0$. In this case, the least importance is allocated to the radar SNR constraint while this constraint is met, so that we have reserved most system DoFs to be used for maximizing the objective of secrecy rate. The closed-form expression based IRS parameter update is summarized as Algorithm 2. Algorithm 2 is called by Algorithm 1 when the IRS parameter needs to be updated in the second sub-problem block in each iteration. The closed-form expression based IRS parameter update method proposed in this section, which invokes quadratic transform [30], is named as ‘‘qtMM’’ for short.

Algorithm 2: qtMM - Update of IRS parameter in $(t + 1)$ -th/current iteration based on proposed closed-form solution based low-complexity scheme in Section IV.

Result: Return $\phi^*(\rho^*)$ as the IRS parameter.

```

if  $g_1(\phi^*(0)) \geq 0$  then
   $\rho^* = 0$ ;
else
   $x = x_{ini}$ ;
  while  $g_1(\phi(2^x)) < 0$  do
     $x = x + 1$ ;
  end
   $\rho_{ub} = 2^x$ ;
   $\rho_{lb} = 2^{x-1}$ ;
   $\rho_{mid} = (\rho_{lb} + \rho_{ub})/2$ ;
  while [ $g_1(\phi(\rho_{mid})) < 0 || g_1(\phi(\rho_{mid})) > \epsilon_{in}$ ] do
    if  $g_1(\phi(\rho_{mid})) < 0$  then
       $\rho_{lb} = \rho_{mid}$ ;
    else
       $\rho_{ub} = \rho_{mid}$ ;
    end
  end
   $\rho_{mid} = (\rho_{lb} + \rho_{ub})/2$ ;
end
   $\rho^* = \rho_{mid}$ ;
end
 $\phi^*(\rho^*) = \exp[j \arg(\mathbf{v}(\rho^*) + \boldsymbol{\kappa}^*(\rho^*))]$ ;

```

V. NUMERICAL RESULTS

In this section, we present numerical results to demonstrate the convergence of the proposed algorithm, its beamforming performance, its secrecy performance, and its advantage in terms of scalability.

While AN helps PLS, it results in loss of communication signal power. We define ω as the ratio of user information power over the total power of user information and AN, and show, via simulations, how ω affects the system performance.

The channels are simulated as Rician fading channels, i.e.,

$$\mathbf{g} = \sqrt{\frac{\kappa_g}{\kappa_g + 1}} \mathbf{g}_{los} + \sqrt{\frac{1}{\kappa_g + 1}} \mathbf{g}_{nlos}, \quad (54)$$

TABLE I
SYSTEM CONFIGURATIONS

Parameter	Value
Error tolerance indicator of Algorithm 1, ϵ [dB]	-20
Maximum number of iterations allowed, t_{max}	15
Rician factors of \mathbf{g} , \mathbf{f} , \mathbf{H}_{dl} , and \mathbf{H}_{ul} [dB]	20
Noise power at the radar receiver, σ_{te}^2 [dBm]	0
Noise power at the communication user, σ_u^2 [dBm]	0
Noise power at the target/ED, σ_{te}^2 [dBm]	0
Inter-antenna distance at radar transmitter/receiver, d	$\lambda/2$
Number of antennas of radar transmitter, N_T	16
Number of antennas of radar receiver, N_R	16
Number of IRS elements, N	64
Target coefficient $ \beta $ [dB]	-40
SNR threshold at radar receiver $\gamma_{R,th}$ [dB]	-11
Radar power budget P_R [dBm]	30
Elevation and azimuth angles of target relative to IRS (ψ_e, ψ_a)	$(60^\circ, 30^\circ)$
Elevation and azimuth angles of user relative to IRS	$(-45^\circ, -45^\circ)$
Azimuth angle of user relative to radar	-30°
Azimuth angle of IRS relative to radar	60°
CSI error level	0

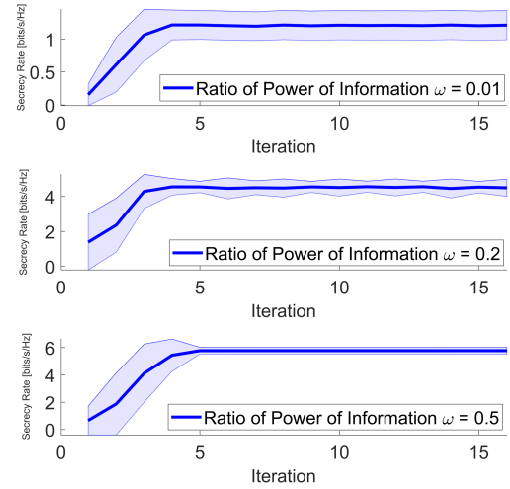


Fig. 2. Convergence of the proposed algorithm when the ratio of information power ω varies.

where $\mathbf{g}_{los} \in \mathbb{C}^{N_T \times 1}$, $\mathbf{g}_{nlos} \in \mathbb{C}^{N_T \times 1}$, and κ_g are respectively the LoS component, NLoS component and Rician factor of \mathbf{g} . The channels \mathbf{f} , \mathbf{H}_{ul} and \mathbf{H}_{dl} are similarly defined. The parameters of the simulation are taken as shown as in Table I unless otherwise stated.

Convergence - Fig. 2 demonstrates the convergence of our proposed algorithm. The solid blue line represents the mean of the objective (secrecy rate) versus iteration number, obtained based 100 different channel realizations. The light blue shaded area around the solid line shows the variance among the realizations. From the figure one can see that the objective, $R_u - R_{te}$, reaches convergence very fast for a wide range of values of ω .

Secrecy performance versus ω - Fig. 3 shows the effect of the power ratio of user information, ω , on the achievable rates. When ω is small, low power is allocated to the user information, and high power to the AN. As a result, the user rate (R_u) and rate at the target/ED (R_{te}) are both low, and

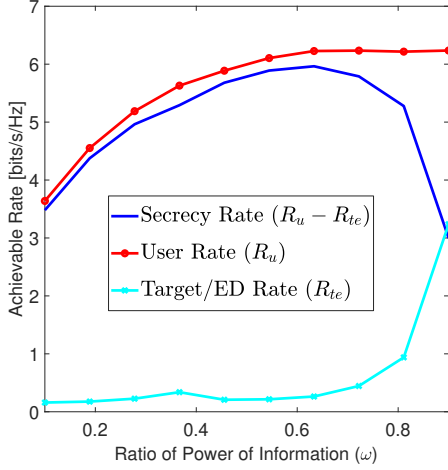


Fig. 3. The impact of ω on the achievable rates.

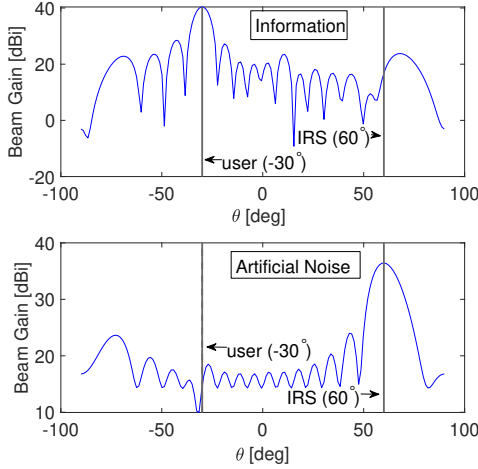


Fig. 4. First subplot: radar beampattern contributed by the waveform which contains the information intended for the user; Second subplot: radar beampattern contributed by the AN; $\omega = 0.7$, Rician factors: 20 dB.

the secrecy rate ($R_u - R_{te}$) is also low. As ω increases, both R_u and R_{te} increase. R_u increases fast when ω is small, and slower when ω is large. Meanwhile, R_{te} rises slowly when ω is low, and increases fast when ω is large. Therefore, with the increase of ω , the secrecy rate, $R_u - R_{te}$, increases at first, since R_u increases faster than R_{te} in the beginning (See Fig. 3 when ω is less than 0.6). Afterwards, R_{te} rises faster, so the secrecy rate drops. When ω is close to 1, the waveform sent to illuminate the target/ED for the sensing task primarily consists of user information, which leads to high ED rate, and decreased secrecy rate.

Beampatterns under dominant LoS channel component - Fig. 4 shows the radar beampatterns respectively contributed by the radar waveform that contains the user information and the AN. Fig. 5 displays the IRS beampattern. Here, we set $\omega = 0.7$ and $N = 64$. The Rician factors of channels \mathbf{g} , \mathbf{f} , \mathbf{H}_{dl} are 20 dB, so the LoS components are dominant. It can be seen from Fig. 4 that, at the radar, the information bearing signal forms a beam to the direction of the user, and the AN forms one towards the IRS. In addition, the IRS forms a beam to the target, per

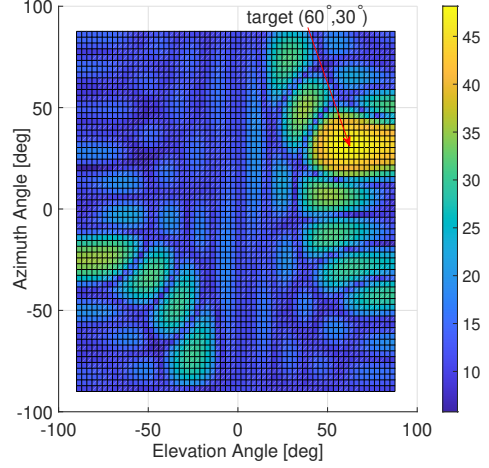


Fig. 5. Obtained IRS beampattern; $\omega = 0.7$, Rician factors: 20 dB.

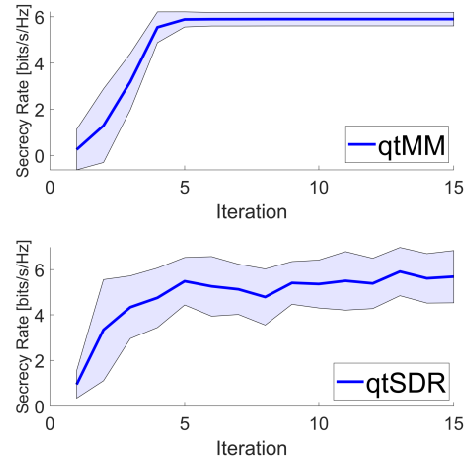


Fig. 6. The proposed closed-form expression based IRS parameter update scheme (qtMM) versus the one in [1] (qtSDR).

Fig. 5. Therefore, by our design, the AN is directed towards the IRS, and upon reflections is directed by the IRS towards the target/ED to simultaneously illuminate and jam it.

Performance comparison with qtSDR - Fig. 6 shows the convergence of the proposed qtMM and that of qtSDR. Here we set $N = 36$ and $\omega = 0.5$. It is observed that the qtMM achieves higher secrecy performance and exhibits less variance during the iterations. For both methods, the numbers of iterations to achieve convergence are around 5. Moreover, for an IRS size $N = 36$ on average qtMM takes around 6.6 seconds to achieve convergence, while the qtSDR needs 50 seconds.

Let's characterize the feasible rate as the likelihood that the solution obtained for the IRS parameter in the second subproblem meets the radar SNR constraint, i.e. $\gamma_R(\phi) \geq \gamma_{R,th}$. Fig. 7 describes the feasible rates of the solved IRS parameter for $N = 25$. For the qtSDR, a randomly generated solution, obtained by Gaussian randomization, that statistically attains a good secrecy rate does not necessarily satisfy the radar SNR constraint in Eq. (40d). In addition, as the radar SNR threshold

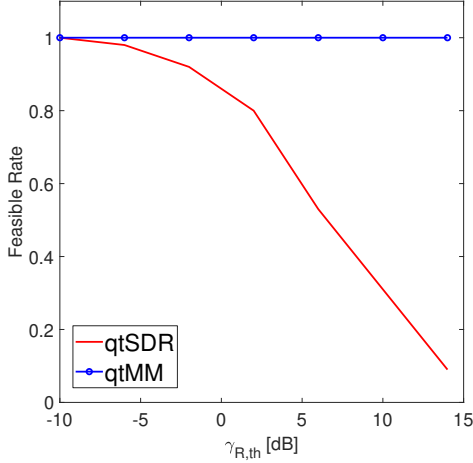


Fig. 7. Feasible rates of the proposed methods in the second sub-problem.

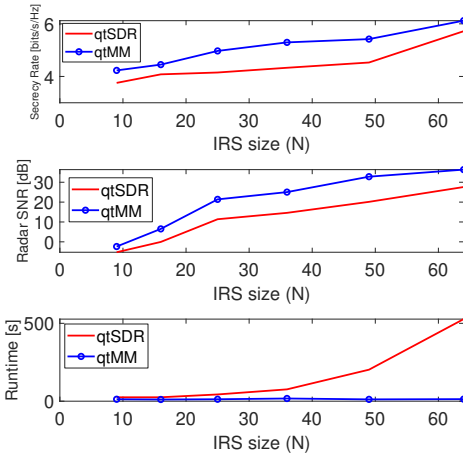


Fig. 8. Comparison between proposed qtMM and qtSDR when the IRS size (N) varies.

$\gamma_{R,th}$ increases, the radar SNR constraint is less likely to be satisfied. For example, when $\gamma_{R,th} = -6$ dB, the feasible rate of qtSDR, or the probability that the SNR constraint (40d) is satisfied, is 98%. When $\gamma_{R,th} = 10$ dB, the feasible rate of qtSDR decreases to 31%. In addition, the feasible rate of qtMM stays at 100% as $\gamma_{R,th}$ changes. The explanation is as follows. When $\gamma_{R,th}$ increases, meaning that there is a more strict constraint on the SNR at the radar receiver, the qtMM increases the importance factor (ρ) of the radar SNR constraint (48c) until it is satisfied.

Fig. 8 compares the qtSDR and the proposed qtMM in terms of secrecy rate, radar receiver SNR and average runtime of convergence, as the size of IRS (N) changes. From the first subplot, it is observed that the qtMM obtains better secrecy rate than the qtSDR, and further achieves better radar SNR per the second subplot. As shown in the third subplot, while in the low N regime, the average runtimes of the qtMM and the qtSDR are similar, the average runtime of the qtSDR increases fast with the IRS size (N). The average runtime of qtMM stays around 10 seconds for N ranging from 9 to 64.

Performance using imperfect channel state information (CSI)

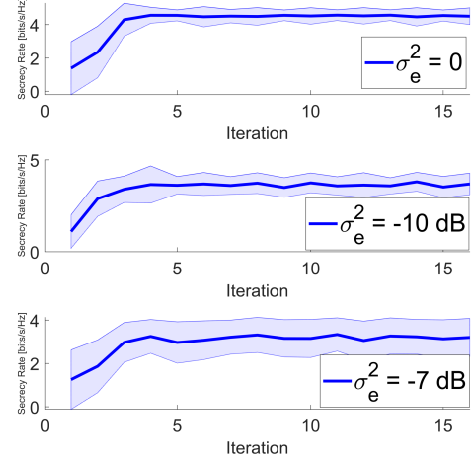


Fig. 9. Convergence of the proposed algorithm for different CSI error levels.

- The channel estimates will always contain some level of estimation error. On denoting the n -th element of the true channel \mathbf{g} by g_n , and the estimated one by \hat{g}_n , we can write

$$g_n = \hat{g}_n + \epsilon_{g_n}, \quad (55)$$

where $\epsilon_{g_n} \sim \mathcal{CN}(0, \frac{\sigma_e^2 \zeta_g}{\kappa_g + 1})$ is the channel error with ζ_g being the large-scale fading coefficient of the channel \mathbf{g} ; $\hat{g}_n \sim \mathcal{CN}(\sqrt{\frac{\kappa_g}{\kappa_g + 1}} g_{los,n}, \frac{1 - \sigma_e^2}{1 + \kappa_g} \zeta_g)$ where $g_{los,n}$ is the n -th element of \mathbf{g}_{los} . In addition, ϵ_{g_n} and \hat{g}_n are independent with each other. The imperfect CSI models for \mathbf{f} , \mathbf{H}_{ul} and \mathbf{H}_{dl} are defined likewise.

Fig. 9 shows the convergence of our proposed algorithm as the CSI error level σ_e^2 varies. In these experiments, $\omega = 0.2$, and the Rician factor of the channels are set to 0 dB. Fig. 9 shows that in all three sub-figures, our proposed method can achieve convergence in a few iterations. As expected, higher CSI error level results in lower secrecy rate. For example, compared to the $\sigma_e^2 = 0$ case where genie-aided perfect CSI is available, the secrecy rates of $\sigma_e^2 = -10$ dB case and $\sigma_e^2 = -7$ dB case are decreased by 19% and 30%, respectively. When the Rician factors are 0 dB, our proposed qtMM achieves convergence even if σ_e^2 is as large as -0.04 dB (dimensionless value of 0.99). The secrecy rate is around 1 bits/s/Hz in that case.

Figs. 10 and 11 illustrate the effect of CSI error on the IRS beampattern where $\omega = 0.5$ and the Rician factors of the channels are set as -20 dB. When CSI error is present, the gain of the main lobe towards the target is decreased by 4.5 dB by comparing Figs. 10 and 11. In addition, side lobes appear when CSI error exists, as Fig. 11 shows. When the Rician factors are set as -20 dB, our proposed qtMM achieves quite stable convergence when σ_e^2 is smaller than -3 dB (the dimensionless value of 0.50).

VI. CONCLUSIONS

In this paper, we have considered an IRS-aided DFRC system, where the target to be sensed acts as an eavesdropper.

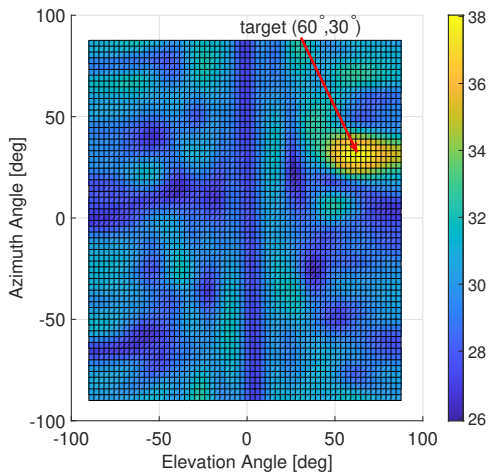


Fig. 10. Obtained IRS beampattern; $\omega = 0.5$, Rician factors: -20 dB, $\sigma_e^2 = 0$.

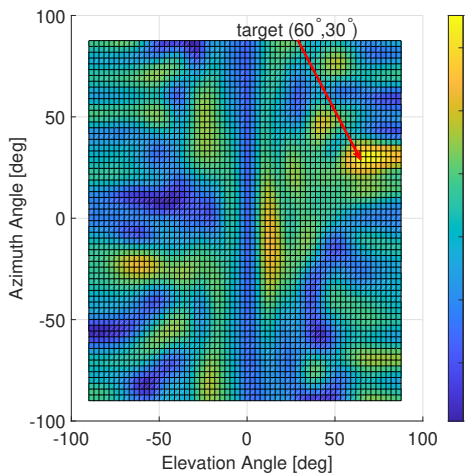


Fig. 11. Obtained IRS beampattern; $\omega = 0.5$, Rician factors: -20 dB, $\sigma_e^2 = -3$ dB.

We have proposed an alternating optimization algorithm to jointly design the transmitted information bearing waveform, the AN, and the IRS parameter matrix, aiming to maximize the secrecy rate subject to certain non-convex constraints. We have invoked an efficient fractional programming technique and a quadratic transform to convert the fractional objective of secrecy rate into to a more mathematically tractable non-fractional form. Thereby, the design of the waveform and the AN was transformed into a non-fractional quadratic programming problem. The IRS design problem, which contains a challenging fourth order function of the IRS parameter, was reduced into a linear order one by applying the effective bounding technique, MM, twice. The other quadratic functions of the IRS parameter were downgraded to linear terms via MM. The transformed problem was solved by solving its dual, which admits a low-complexity closed-form expression solution. Numerical results are presented to illustrate the convergence properties of the proposed system design method, as well as the secrecy rate and beamforming performance of the designed system.

APPENDIX A

DERIVATION OF LAGRANGIAN DUAL EXPRESSIONS OF R_u AND R_{te} AS (10) AND (11)

At first, we show a universal method for converting a function containing multiple fractional terms, to non-fractional form. Assume an objective is the addition of I terms as [30]

$$f(\mathbf{x}) = \sum_{i=1}^I \omega_i \log(1 + A_i(\mathbf{x})/B_i(\mathbf{x})), \quad (56)$$

where \mathbf{x} is the variable to be optimized, ω_i is the weight factor for the i -th term, $A_i(\mathbf{x})$ and $B_i(\mathbf{x})$ are polynomials of \mathbf{x} for $i \in \{1, \dots, I\}$. Then $f(\mathbf{x})$ can be transformed via Lagrangian dual reformulation as

$$f(\mathbf{x}, \boldsymbol{\gamma}) = \sum_{i=1}^I \omega_i \log(1 + \gamma_i) - \sum_{i=1}^I \omega_i \gamma_i + \sum_{i=1}^I \omega_i (1 + \gamma_i) \frac{A_i(\mathbf{x})}{A_i(\mathbf{x}) + B_i(\mathbf{x})}, \quad (57)$$

where $\boldsymbol{\gamma} = [\gamma_1, \dots, \gamma_i, \dots, \gamma_I]^T$ is an auxiliary variable where γ_i can be optimally updated as

$$\gamma_i^* = A_i(\mathbf{x})/B_i(\mathbf{x}), \quad \forall i = 1, \dots, I \quad (58)$$

The optimal γ_i^* above can be easily obtained by taking \mathbf{x} as a constant and letting $\partial f(\boldsymbol{\gamma})/\partial \gamma_i = 0$. To make the objective be non-fractional, we apply quadratic transform to the third term of the objective as

$$f(\mathbf{x}, \boldsymbol{\gamma}) \rightarrow f(\mathbf{x}, \boldsymbol{\gamma}, \mathbf{y}) = \sum_{i=1}^I \omega_i \log(1 + \gamma_i) - \sum_{i=1}^I \omega_i \gamma_i + \sum_{i=1}^I 2y_i \sqrt{\omega_i (1 + \gamma_i) A_i(\mathbf{x})} - \sum_{i=1}^I y_i^2 (A_i(\mathbf{x}) + B_i(\mathbf{x})), \quad (59)$$

where $\mathbf{y} = [y_1, \dots, y_i, \dots, y_I]^T$ is an auxiliary variable and can be updated as

$$y_i = \sqrt{\omega_i (1 + \gamma_i) A_i(\mathbf{x})} / (A_i(\mathbf{x}) + B_i(\mathbf{x})), \quad \forall i = 1, \dots, I \quad (60)$$

By applying the aforementioned method, the fractional function R_u in (6) is converted to a non-fractional function as (10). Specifically, we replace the variable \mathbf{x} with \mathbf{w} and \mathbf{W}_n , and we let $I = 1$, $\omega_1 = 1$, $A_1(\mathbf{w}, \mathbf{W}_n) = |\mathbf{c}_u^T \mathbf{w}|^2$, $B_1(\mathbf{w}, \mathbf{W}_n) = \|\mathbf{c}_u^T \mathbf{W}_n\|^2 + \sigma_u^2$. Note that γ_u and α_u in (10) respectively correspond to γ_1 and y_1 in (59). Similarly, by letting $A_1(\mathbf{w}, \mathbf{W}_n) = |\mathbf{c}_{te}^T \mathbf{w}|^2$, $B_1(\mathbf{w}, \mathbf{W}_n) = \|\mathbf{c}_{te}^T \mathbf{W}_n\|^2 + \sigma_{te}^2$, R_{te} in (7) is converted to a non-fractional function as (11).

APPENDIX B

DERIVATION OF UPDATE OF IRS PARAMETER VECTOR IN QTMM

The Lagrangian multiplier ρ , is omitted for the sake of exposition, i.e. $\phi(\rho)$ is written as ϕ without affecting the results. By invoking

$$g_0(\phi) = \phi_t^T (\mathbf{L}_1 + \bar{\mathbf{L}}_1) \phi^* + \phi^T (\mathbf{L}_1 + \bar{\mathbf{L}}_1) \phi_t^* - \phi_t^T (\mathbf{L}_1 + \bar{\mathbf{L}}_1) \phi_t^* + \Re[\phi^T (\boldsymbol{\eta} - \boldsymbol{\mu} - \bar{\boldsymbol{\mu}})], \\ g_1(\phi) = 2\phi_t^H \mathbf{L}_2 \phi^* - \phi_t^H \mathbf{L}_2 \phi_t^* + 2\phi_t^T \mathbf{L}_3 \phi - \phi_t^T \mathbf{L}_3 \phi_t - \gamma'_{R,th} \quad (61)$$

we have

$$\Re[g_0(\phi) + \rho g_1(\phi)] = \Re[\boldsymbol{\nu}^T \phi^* + \boldsymbol{\kappa}^T \phi + c_L], \quad (62)$$

where $\boldsymbol{\nu}$ and $\boldsymbol{\kappa}$ are respectively expressed as (52) and (53), and c_L is a constant not relevant to ϕ as

$$c_L = -\phi_t^T (\mathbf{L}_1 + \bar{\mathbf{L}}_1) \phi_t^* - \rho(\gamma_{R,th} + \phi_t^H \mathbf{L}_2 \phi_t^* + \phi_t^T \mathbf{L}_3 \phi_t), \quad (63)$$

where ϕ_t is the solved solution of ϕ in t -th/previous iteration and t is the index of outer iteration in Algorithm 1. c_L can be dropped safely. The term $\Re[\boldsymbol{\nu}^T \phi^*]$ in (62) can be written as

$$\begin{aligned} \Re[\boldsymbol{\nu}^T \phi^*] &= \Re\{(\Re[\boldsymbol{\nu}^T] + j\Im[\boldsymbol{\nu}^T])(\Re[\phi] - j\Im[\phi])\} \\ &= \Re[\boldsymbol{\nu}^T] \Re[\phi] + \Im[\boldsymbol{\nu}^T] \Im[\phi]. \end{aligned} \quad (64)$$

In addition, a term $\Re[\boldsymbol{\nu}^H \phi]$ can be also expressed as

$$\begin{aligned} \Re[\boldsymbol{\nu}^H \phi] &= \Re\{(\Re[\boldsymbol{\nu}^T] - j\Im[\boldsymbol{\nu}^T])(\Re[\phi] + j\Im[\phi])\} \\ &= \Re[\boldsymbol{\nu}^T] \Re[\phi] + \Im[\boldsymbol{\nu}^T] \Im[\phi]. \end{aligned} \quad (65)$$

Obviously

$$\Re[\boldsymbol{\nu}^T \phi^*] = \Re[\boldsymbol{\nu}^H \phi]. \quad (66)$$

Therefore the first two terms in (62) can be written as

$$\Re[\boldsymbol{\nu}^T \phi^* + \boldsymbol{\kappa}^T \phi] = \Re[\boldsymbol{\nu}^H \phi + \boldsymbol{\kappa}^T \phi] = \Re[(\boldsymbol{\nu}^H + \boldsymbol{\kappa}^T) \phi]. \quad (67)$$

According to [49], to maximize $\Re[\mathbf{a}^H \phi]$ where $\mathbf{a} \in \mathbb{C}^{N \times 1}$, the phase of the n -th element of \mathbf{a} and that of ϕ should be equal $\forall n \in \{1, \dots, N\}$, i.e.

$$\begin{aligned} \phi &= [\exp(j \arg[a_1]), \dots, \exp(j \arg[a_N])]^T \\ &= \exp(j \arg[\mathbf{a}]). \end{aligned} \quad (68)$$

Likewise, the ϕ that maximize $\Re[(\boldsymbol{\nu}^H + \boldsymbol{\kappa}^T) \phi]$ is

$$\phi = \exp[j \arg[(\boldsymbol{\nu}^H + \boldsymbol{\kappa}^T)^H]] = \exp[j \arg(\boldsymbol{\nu} + \boldsymbol{\kappa}^*)]. \quad (69)$$

REFERENCES

- [1] Y.-K. Li and A. Petropulu, "An IRS-assisted secure dual-function radar-communication system," *arXiv:2310.00555*, 2023.
- [2] X. Chen, Z. Feng, Z. Wei, F. Gao, and X. Yuan, "Performance of joint sensing-communication cooperative sensing UAV network," *IEEE Trans. Veh. Technol.*, vol. 69, no. 12, pp. 15 545–15 556, 2020.
- [3] Z. Feng, Z. Fang, Z. Wei, X. Chen, Z. Quan, and D. Ji, "Joint radar and communication: A survey," *China Commun.*, vol. 17, no. 1, pp. 1–27, 2020.
- [4] J. A. Zhang, F. Liu, C. Masouros, R. W. Heath, Z. Feng, L. Zheng, and A. Petropulu, "An overview of signal processing techniques for joint communication and radar sensing," *IEEE Journal of Selected Topics in Signal Processing*, vol. 15, no. 6, pp. 1295–1315, 2021.
- [5] C. Sturm and W. Wiesbeck, "Waveform design and signal processing aspects for fusion of wireless communications and radar sensing," *Proc. IEEE*, vol. 99, no. 7, pp. 1236–1259, 2011.
- [6] J. Mu, R. Zhang, Y. Cui, N. Gao, and X. Jing, "UAV meets integrated sensing and communication: Challenges and future directions," *IEEE Commun. Mag.*, vol. 61, no. 5, pp. 62–67, 2023.
- [7] T. Ma, Y. Xiao, X. Lei, and M. Xiao, "Integrated sensing and communication for wireless extended reality (XR) with reconfigurable intelligent surface," *IEEE J. Sel. Topics Signal Process.*, vol. 17, no. 5, pp. 980–994, 2023.
- [8] X. Zhao and Y.-J. A. Zhang, "Joint beamforming and scheduling for integrated sensing and communication systems in URLLC," in *GLOBECOM 2022 - 2022 IEEE Global Communications Conference*, 2022, pp. 3611–3616.
- [9] Y. Zhong, T. Bi, J. Wang, J. Zeng, Y. Huang, T. Jiang, Q. Wu, and S. Wu, "Empowering the V2X network by integrated sensing and communications: Background, design, advances, and opportunities," *IEEE Netw.*, vol. 36, no. 4, pp. 54–60, 2022.
- [10] F. Liu, C. Masouros, A. P. Petropulu, H. Griffiths, and L. Hanzo, "Joint radar and communication design: Applications, state-of-the-art, and the road ahead," *IEEE Trans. Commun.*, vol. 68, no. 6, pp. 3834–3862, 2020.
- [11] A. Hassaniien, M. G. Amin, E. Aboutanios, and B. Himed, "Dual-function radar communication systems: A solution to the spectrum congestion problem," *IEEE Signal Process. Mag.*, vol. 36, no. 5, pp. 115–126, 2019.
- [12] D. Ma, N. Shlezinger, T. Huang, Y. Liu, and Y. C. Eldar, "Joint radar-communication strategies for autonomous vehicles: Combining two key automotive technologies," *IEEE Signal Process. Mag.*, vol. 37, no. 4, pp. 85–97, 2020.
- [13] A. D. Wyner, "The wire-tap channel," *The Bell System Technical Journal*, vol. 54, no. 8, pp. 1355–1387, 1975.
- [14] S. A. A. Fakoorian and A. L. Swindlehurst, "Solutions for the MIMO gaussian wiretap channel with a cooperative jammer," *IEEE Trans. Signal Process.*, vol. 59, no. 10, pp. 5013–5022, 2011.
- [15] L. Dong, Z. Han, A. P. Petropulu, and H. V. Poor, "Improving wireless physical layer security via cooperating relays," *IEEE Trans. Signal Process.*, vol. 58, no. 3, pp. 1875–1888, 2010.
- [16] G. Zheng, L.-C. Choo, and K.-K. Wong, "Optimal cooperative jamming to enhance physical layer security using relays," *IEEE Trans. Signal Process.*, vol. 59, no. 3, pp. 1317–1322, 2011.
- [17] J. Li, A. P. Petropulu, and S. Weber, "On cooperative relaying schemes for wireless physical layer security," *IEEE Trans. Signal Process.*, vol. 59, no. 10, pp. 4985–4997, 2011.
- [18] G. Zheng, I. Krikidis, J. Li, A. P. Petropulu, and B. Ottersten, "Improving physical layer secrecy using full-duplex jamming receivers," *IEEE Trans. Signal Process.*, vol. 61, no. 20, pp. 4962–4974, 2013.
- [19] A. Khisti and G. W. Wornell, "Secure transmission with multiple antennas I: The MISOME wiretap channel," *IEEE Trans. Inf. Theory*, vol. 56, no. 7, pp. 3088–3104, 2010.
- [20] S. Goel and R. Negi, "Guaranteeing secrecy using artificial noise," *IEEE Trans. Wireless Commun.*, vol. 7, no. 6, pp. 2180–2189, 2008.
- [21] N. Su, F. Liu, C. Masouros, T. Ratnarajah, and A. Petropulu, "Secure dual-functional radar-communication transmission: Hardware-efficient design," in *2021 55th Asilomar Conference on Signals, Systems, and Computers*, 2021, pp. 629–633.
- [22] N. Su, F. Liu, and C. Masouros, "Sensing-assisted eavesdropper estimation: An ISAC breakthrough in physical layer security," *arXiv:2210.08286*, 2023.
- [23] T. Wei, L. Wu, K. V. Mishra, and M. R. B. Shankar, "Multiple IRS-assisted wideband dual-function radar-communication," in *2022 2nd IEEE International Symposium on Joint Communications & Sensing (JC&S)*, 2022, pp. 1–5.
- [24] Z.-M. Jiang, M. Rihan, P. Zhang, L. Huang, Q. Deng, J. Zhang, and E. M. Mohamed, "Intelligent reflecting surface aided dual-function radar and communication system," *IEEE Syst. J.*, pp. 1–12, 2021.
- [25] Y. Li and A. Petropulu, "Dual-function radar-communication system aided by intelligent reflecting surfaces," in *2022 IEEE 12th Sensor Array and Multichannel Signal Processing Workshop (SAM)*, 2022, pp. 126–130.
- [26] Y.-K. Li and A. Petropulu, "Minorization-based low-complexity design for IRS-aided ISAC systems," in *2023 IEEE Radar Conference (Radar-Conf23)*, 2023, pp. 1–6.
- [27] R. Liu, M. Li, Y. Liu, Q. Wu, and Q. Liu, "Joint transmit waveform and passive beamforming design for RIS-aided DFRC systems," *IEEE J. Sel. Topics Signal Process.*, vol. 16, no. 5, pp. 995–1010, 2022.
- [28] Y.-K. Li and A. Petropulu, "Intelligent reflecting surface-assisted dual-function radar-communication system," *IEEE Access*, pp. 1–1, 2023.
- [29] Y. Sun, P. Babu, and D. P. Palomar, "Majorization-minimization algorithms in signal processing, communications, and machine learning," *IEEE Trans. Signal Process.*, vol. 65, no. 3, pp. 794–816, 2017.
- [30] K. Shen and W. Yu, "Fractional programming for communication systems—part I: Power control and beamforming," *IEEE Trans. Signal Process.*, vol. 66, no. 10, pp. 2616–2630, 2018.
- [31] M. Najafi, V. Jamali, R. Schober, and H. V. Poor, "Physics-based modeling and scalable optimization of large intelligent reflecting surfaces," *IEEE Trans. Commun.*, vol. 69, no. 4, pp. 2673–2691, 2021.
- [32] Y.-K. Li and A. Petropulu, "Efficient beamforming designs for IRS-aided DFRC systems," in *2023 24th International Conference on Digital Signal Processing (DSP)*, 2023, pp. 1–5.
- [33] X. He and J. Wang, "QCQP with extra constant modulus constraints: Theory and application to SINR constrained mmwave hybrid beamforming," *IEEE Trans. Signal Process.*, vol. 70, pp. 5237–5250, 2022.

- [34] C. Wang, C.-C. Wang, Z. Li, D. W. K. Ng, K.-K. Wong, N. Al-Dhahir, and D. Niyato, "STAR-RIS-enabled secure dual-functional radar-communications: Joint waveform and reflective beamforming optimization," *IEEE Trans. Inf. Forensics Security*, vol. 18, pp. 4577–4592, 2023.
- [35] M. Hua, Q. Wu, W. Chen, O. A. Dobre, and A. Lee Swindlehurst, "Secure intelligent reflecting surface aided integrated sensing and communication," *IEEE Trans. Wireless Commun.*, pp. 1–1, 2023.
- [36] J. Chu, Z. Lu, R. Liu, M. Li, and Q. Liu, "Joint beamforming and reflection design for secure RIS-ISAC systems," *IEEE Trans. Veh. Technol.*, pp. 1–5, 2023.
- [37] H. Zhang and J. Zheng, "IRS-assisted secure radar communication systems with malicious target," *IEEE Trans. Veh. Technol.*, pp. 1–14, 2023.
- [38] S. Sweta, A. Dubey, and V.-L. Nguyen, "Efficient IRS-aided rate optimizations for dual functional radar and communications," *IEEE Commun. Lett.*, pp. 1–1, 2023.
- [39] H. Zhao, F. Wu, W. Xia, Y. Zhang, Y. Ni, and H. Zhu, "Joint beamforming design for RIS-aided secure integrated sensing and communication systems," *IEEE Commun. Lett.*, vol. 27, no. 11, pp. 2943–2947, 2023.
- [40] A. A. Salem, M. H. Ismail, and A. S. Ibrahim, "Active reconfigurable intelligent surface-assisted MISO integrated sensing and communication systems for secure operation," *IEEE Trans. Veh. Technol.*, pp. 1–13, 2022.
- [41] K. V. Mishra, A. Chattopadhyay, S. S. Acharjee, and A. P. Petropulu, "Optm3sec: Optimizing multicast IRS-aided multi-antenna DFRC secrecy channel with multiple eavesdroppers," in *ICASSP 2022 - 2022 IEEE International Conference on Acoustics, Speech and Signal Processing (ICASSP)*, 2022, pp. 9037–9041.
- [42] W. Dinkelbach, "On nonlinear fractional programming," *Management Science*, vol. 13, no. 7, pp. 492–498, 1967.
- [43] S. Evmorfos, A. P. Petropulu, and H. V. Poor, "Actor-critic methods for IRS design in correlated channel environments: A closer look into the neural tangent kernel of the critic," *IEEE Trans. Signal Process.*, vol. 71, pp. 4029–4044, 2023.
- [44] Q. Liu, Y. Zhu, M. Li, R. Liu, Y. Liu, and Z. Lu, "DRL-based secrecy rate optimization for RIS-assisted secure ISAC systems," *IEEE Trans. Veh. Technol.*, pp. 1–5, 2023.
- [45] S. Jiang and A. Alkhateeb, "Sensing aided OTFS massive MIMO systems: Compressive channel estimation," in *2023 IEEE International Conference on Communications Workshops (ICC Workshops)*, 2023, pp. 794–799.
- [46] S. Mura, M. Mizmizi, U. Spagnolini, and A. Petropulu, "Enhanced channel estimation in mm-wave MIMO systems leveraging integrated communication and sensing," *arXiv:2309.14875*, 2023.
- [47] B. Li and A. P. Petropulu, "Joint transmit designs for coexistence of MIMO wireless communications and sparse sensing radars in clutter," *IEEE Trans. Aerosp. Electron. Syst.*, vol. 53, no. 6, pp. 2846–2864, 2017.
- [48] M. Grant and S. Boyd, "CVX: Matlab software for disciplined convex programming, version 2.1," <http://cvxr.com/cvx>, Mar. 2014.
- [49] H. Shen, W. Xu, S. Gong, Z. He, and C. Zhao, "Secrecy rate maximization for intelligent reflecting surface assisted multi-antenna communications," *IEEE Commun. Lett.*, vol. 23, no. 9, pp. 1488–1492, 2019.